History of Medicine, 2023, 9(1): 2394–2401
DOI: 10.17720/2409-5834.v9.1.2023.309

Effects of AuNPs capped gelatin and photodynamic of laser on evaluation of response in superficial skin tumors in laboratory mice

Entidhar Jasim Khamees[1*], Esraa Fareed Saeed[2]

1Department of Physiology and medical physics, College of Medicine, University of Babylon/Iraq
2Department of science ,Physics and Earth Sciences Curriculum Division, , General Directorate of Curriculum Ministry of Education/Iraq
Email: intdher071@gmail.com

***Correspondence author:** Entidhar Jasim Khamees (intdher071@gmail.com)

Received: 23 February 2023 **Accepted:** 15 May 2023

Citation: Khamees EJ, Saeed EF (2023) Effects of AuNPs capped gelatin and photodynamic of laser on evaluation of response in superficial skin tumors in laboratory mice. History of Medicine 9(1): 2394–2401. https://doi.org/10.17720/2409-5834.v9.1.2023.309

Abstract

Prepared gold nanoparticles and covered with gelatin were synthesized with little difference in gelatin concentration by reducing the volume of a chloric acid stock solution with a fixed volume of sodium citrate dihydrate (34 mm) solution. The nanoparticles had excellent colloidal stability, and TEM revealed the formation of well-spherical gold nanoparticles (AuNPs) of various sizes. The method produces particles with sizes ranging from 10 to 20 nm. The gelatin AuNPs exhibit size-dependent surface Plasmon resonance behavior as measured by UV visible spectroscopy, with SPR ranging from 518 to 543 nm depending on the concentration of gelatin used. The goal of this study is to assess dynamic therapy in vivo using a 532 nm wavelength laser with gelatin-coated gold nanoparticles as photosensitizers. According to the findings of the study, the green diode laser has the best photodynamic therapy effect on cancer cells in vivo after cells photosensitization with gold nanoparticles covered with gelatin at a concentration of 1% and an exposure time of 60 seconds.

Keywords

AuNPs capped gelatin, photodynamic, 532nm laser, laboratory mice, HAuCl4.

Nanoparticles (NPs) have provided significant benefits in terms of improving drug delivery systems by increasing drug effectiveness and efficacy [1][2][3]. In the biological sciences, NPs are submicron particles. NPs offer special and promising qualities in medication delivery systems because of their tiny size [4] . Collage is hydrolyzed to produce the protein known as gelatin. Gelatin nanoparticles have been extensively exploited as gene and medication carriers to target diseased tissues for the treatment of vasospasm and restenosis, as well as cancer, TB, and HIV infection. A biodegradable substance with potential uses in nanobiotechnology and nanopharmaceutics is gelatin. [5][6]

PDT is a minimally invasive technique that has been shown to be effective in the treatment of a variety of tumors. This simple method employs three interdependent components: phototoxic compound (photosensitizer [PS]), light source, and oxygen. [7][8]

Reactive oxygen species (ROS), which are created by photosensitizers once they are triggered with visible or near-infrared light, kill tumor cells in photodynamic therapy (PDT). The efficiency with which the photosensitizer is supplied and the capacity to target are some of the aspects that affect the effectiveness of the PDT[9][10]

Photothermal therapy (PTT) is a promising

biological application in the treatment of cancer because to its low invasiveness, great selectivity, and accuracy. Nanoparticles are frequently utilized as photothermal agents in PTT due to their distinct qualities, such as high photothermal efficiency and tiny diameters that allow tumor penetration (PTA) [11][12]

Because of its special qualities, gold, one of the most precious commodities utilized in daily life, is employed in industries as well as in the production of money, jewelry, accessories, and collectibles. Because of its better electrical conductivity and processing capabilities, gold, for instance, is utilized in semiconductors and as a catalyst in chemical reactions. [13] [14]

Gold has also been used for many years in biological applications. Because of its exceptional physicochemical qualities, gold has been used for in vivo transplants from ancient times. Gold is non-toxic to humans, does not rust, and does not have a bad taste. It can also be shaped into beautiful shapes [13].

An multidisciplinary area of science, engineering, and medicine called cancer nanotechnology has several uses in molecular imaging, diagnostics, and targeted therapy. The fundamental argument is that molecules or crystals lack certain optical, magnetic, or structural qualities that nanometer-sized particles, such semiconductor quantum dots and iron oxide nanocrystals, have[15][16][17].

Experimental section

Materials

Sigma-Aldrich provided the gelatin and HAuCl4.xH2O, Gelatin, Na3C6H5O72H2O (99%). (St. Louis, MO).

Animal model

65 mature Swiss albino female mice weighing 20-25 grams and aged 6-8 weeks were used.The animals were kept in well-ventilated rooms at the animal home.

AuNPs capped gelatin

Nanocomposite sol preparation

Sodium citrate was used as a reducing agent and gelatin as a stabilizing reagent to create gelatin-coated gold particles of varying sizes. 1 Mm of gold solution is added to 34 Mm of sodium citrate solution, and the combination is agitated for 15 minutes until a dark crimson mixture is produced. The heating is turned off when the dark red hue appears. Following that, successive amounts of gelatin solution are added to the red mixture. The mixture was then forcefully mixed for 15 minutes before being left for two hours. Where gold particles were coated with gelatin.

Characterization

Instrumentation used for the results of synthesis of gold nanoparticles-coated gelatin on absorption from surface Plasmon resonance: UV-visible spectroscopy, transmission electron microscopy (TEM).

Transplantation of tumor cells into mice:

In this study, a single tumor-bearing mouse was transplanted into an adult female albino balb/c mouse by means of a stem cell transplant procedure. The transplantation method of (AL-Shamery, 2003)[18] was performed according to the following protocol:

1 ml of tumor cell suspension was transplanted into an adult female albino balb/c mouse through the subcutaneous insertion of a gauge no.18 needle anywhere from the thigh to the shoulder area. Tumor development and measures were evaluated and documented using a plastic Varner caliber [19].

Tumor volume (mm3) = a * b^2 /2

Where a = length of tumor mass (mm), b = width of tumor mass (mm^2)

Experimental grouping:

Thirteen groups of five mice each were created from the animals.

Group 'g1': this group = negativ control (no mammary adenocarcinoma-bearing mice).

Group (G2): this group = control positive (mammary adenocarcinoma-bearing mice).

Group (G3): group injected intratumorally (I/T) (**AuNPs capped gelatin** (1%).

Group (G4): group injected I/T (**AuNPs capped gelatin** 0.50%).

Group (G5) group injected I/T (AuNPs capped gelatin 0.25%).

Group (G6) group injected I/T (AuNPs capped gelatin 0.10%).

Group (G7) group injected I/T (AuNPs) only.
Group (G8): PDT group injected intratumorally (I/T) (**AuNPs capped gelatin** (1%)+laser.
Group (G9): PDT group injected (I/T) (**AuNPs capped gelatin** (0.50%)(1%)+laser..
Group (G10) PDT group injected I/T (AuNPs capped gelatin 0.25%).(1%)+laser.
Group (G11) PDT group injected I/T (AuNPs capped gelatin 0.10%)(1%)+laser..
Group (G12): PDT group injected I/T (AuNPs) only(1%)+laser..
Group (G13) mice having tumors that were exclusively treated with laser.

Delivery of a photosensitizer:

Female mice's thighs were injected subcutaneously with mammary adenocarcinoma cells (AM3).After the tumor has grown to a size of at least 6.5 mm^3, this normally takes 2 weeks. Five tumor-bearing (3,4,5,6, and 7) groups were given AuNPs capped gelatin intra-tumorally at four different concentrations (1 percent ,0.50 percent ,0.25 and 0.1 percent). A 27-gauge needle was used to administer the medication in a 1ml syringe. The treatment was done under general anesthesia with Ketamin (5mg/100gm) + Xylazin (7mg/100gm) injections at several areas of the tumor mass at the same time.

Laser irradiation procedure:

In the physics lab, the procedure of measuring and determining the employed wavelength was carried out utilizing a well-known technique., and detectors manufactured in a laboratory were used to find out the distribution of energy (or power) on the laser beam, and it appeared that the Gaussian distribution, The intensity was then calculated utilizing the connection between the laser power and the measurement of the laser power.

$I = {}^{P}/_{\pi r^2}$.....1

Where **r** it represents the radius and **π** a constant ratio, then we extract the energy density (ED) in units of Joule\cm² using the following relationship.

ED = I * t.....(2)

where **t** represents , λ=532 nm , I= 0.009(W/cm^2) for a 60-minute exposure duration. ED=0.009*60=0.542 Joule\cm²

The therapeutic response was calculated by measuring the tumor volume at weekly intervals for 5 weeks and comparing it to the value at the end of the study (week 0). Throughout the trial, clinical indications such as body weight, anorexia, and anemia were monitored continually following PDT therapy, as well as any changes in the animals' activity or behavior.

After the fifth week, the mice were sacrificed by an overdose of anesthetic and an incision as follows:

Each mouse was attached to the anatomical stage's back and wiped with alcohol (70 percent). An excisional biopsy was performed, which included the tumor mass and the underlying skin, and was fixed in 10% formalin for histological analysis.

To examine how PDT affects the rate of tumor growth inhibition the weekly inhibition rate of tumor growth (GI) was determined using the formula (3)

$GI = \frac{A-B}{A} \times 100$...(3)

GI: stands for growth inhibition, a: for untreated tumor volume, and B: for treated tumor volume.

Results and Discussion

UV–visible spectroscopic analysis

By using UV-visible spectroscopy, the absorption peak in gelatinous AuNPs displayed size-dependent surface Plasmon resonance activity., and the SPR ranged from 518 to 543 nm as shown in figure (1) Represent the absorbance of SPR of AuNPs colors (black) Au ions, color (red) represent the SPR pure AuNPs, color (blue), represent the SPR Au ions and gelatin.

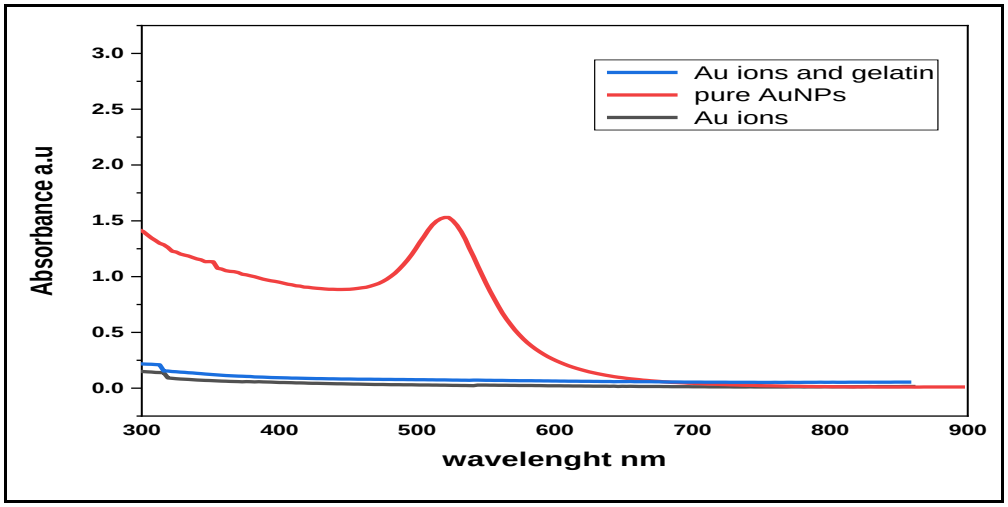

Fig. 1 UV-vis absorption spectra of AuNPs color (black) Au ions, color (red) represent the SPR pure AuNPs, color (blue), represent the SPR Au ions and gelatin

The curves in figure.2 show that the surface Plasmon resonance shifted to the right or red when the volume ratio was raised, and the results are consistent with [5].

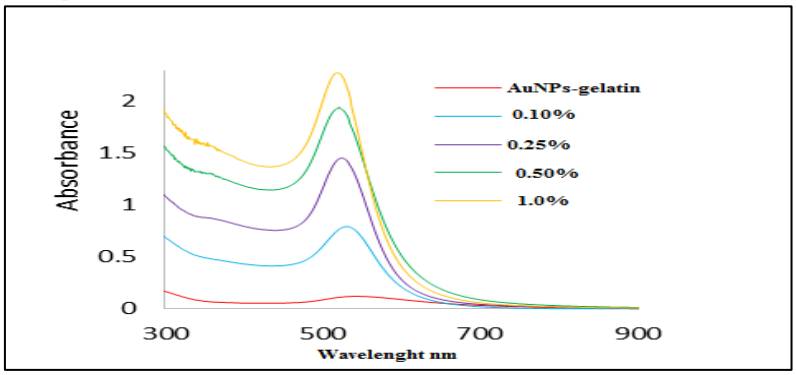

Fig.2 UV-vis absorption spectra of AuNPs stabilized AuNPs at different gelatin concentration (0.1%,0.25%,0.50%,1%).

Transmission Electron Microscopy(TEM):

The TEM images of AuNPs stabilized with varying amounts of gelatin are shown in Figure 3 (0.1%0.25%, 0.50%, and 1%) correspondingly. Depending on the proportion of gelatin containing gold nanoparticles, the particles were spherical and varied somewhat in particle size and size distribution. It was discovered that the prepared with high concentration (1%) had a reduced size as a stabilizing agent. The surface Plasmon band was discovered to emerge around 543 nm. Additionally, it was discovered that the band at the higher value shifted with the reduction in gelatin content, indicating an increase in particle size. The UV-vis absorption measurement shows that the size of the gold nanoparticles, with the exception of pure AuNPs, varied from 20 to 10 nm.In vivo photodynamic treatment results

Clinical manifestations: -including body weight, tumor volume, and the figure for growth inhibition

Control +ve group (G 2) = (Tumor-bearing female mice): The main clinical indicators seen in tumor-bearing female mice were severe anorexia, which resulted in a progressive decrease of body weight, as well as weakness, anemia, and cachexia. All of these symptoms were observed with increasing tumor volume in comparison to control (– ve) G1, as shown in figure (4).

Groups given PDT: In groups (G8, G9, G10, G11, and G12), mice given PDT experienced an increase in body weight that was within a normal range, without any obvious clinical signs. However, animals given AuNPs-capped gelatin only experienced a significant loss in body weight at the third, fourth, and fifth concentrations (1%, 0.50%, 0.25%, and 0. 10%).

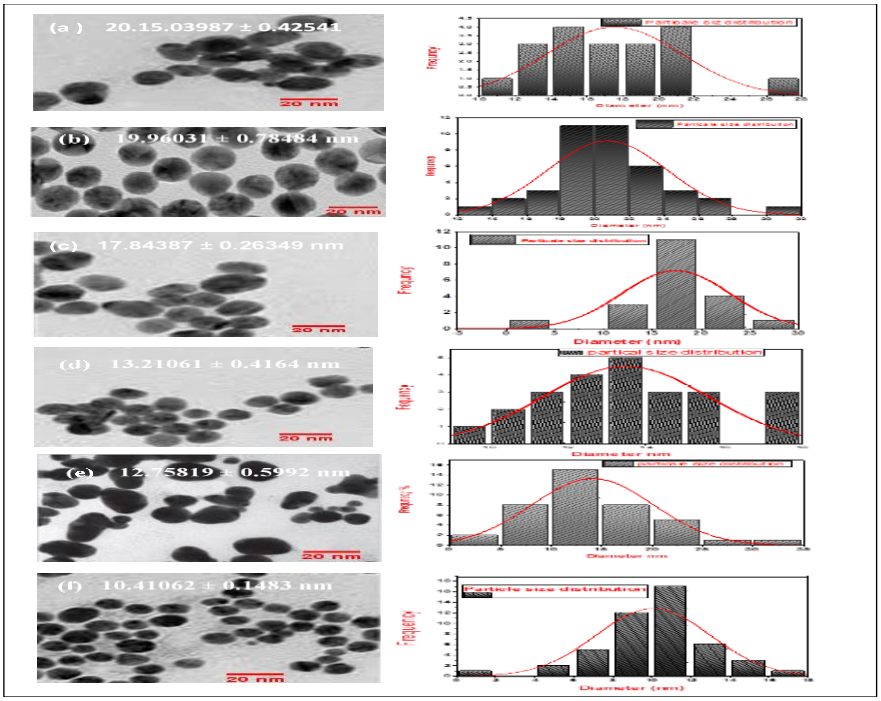

Fig.3 TEM micrographs and Particle size distribution of (a) pure AuNPs, and stabilized AuNPs at different gelatin concentration (c) 0.1%, (d) 0.25%, (e) 0.50% and (f) 1%)

Groups given AuNPs-capped gelatin: At the first and second weeks following intratumoral injection of AuNPs-capped gelatin with different concentrations, there was no significant difference in body weight between tumor-bearing mice treated with different concentrations of ANPs-capped gelatin (1 percent,0.50 percent,0.25 percent,0. 10%), but there was a significant difference in the final three weeks of the experiment, as shown in figure (4)

Groups given gelatin capped with AuNPs: Only at the third week following I/T administration of AuNPs-capped gelatin alone did tumor volume show a significant decline at the level of significance (P 0.05); no macroscopic inhibition was seen at the fifth week following AuNPs-capped gelatin application for any concentration (1%, 0.50%, 0.25%, or 0. 10%), Figure (4).

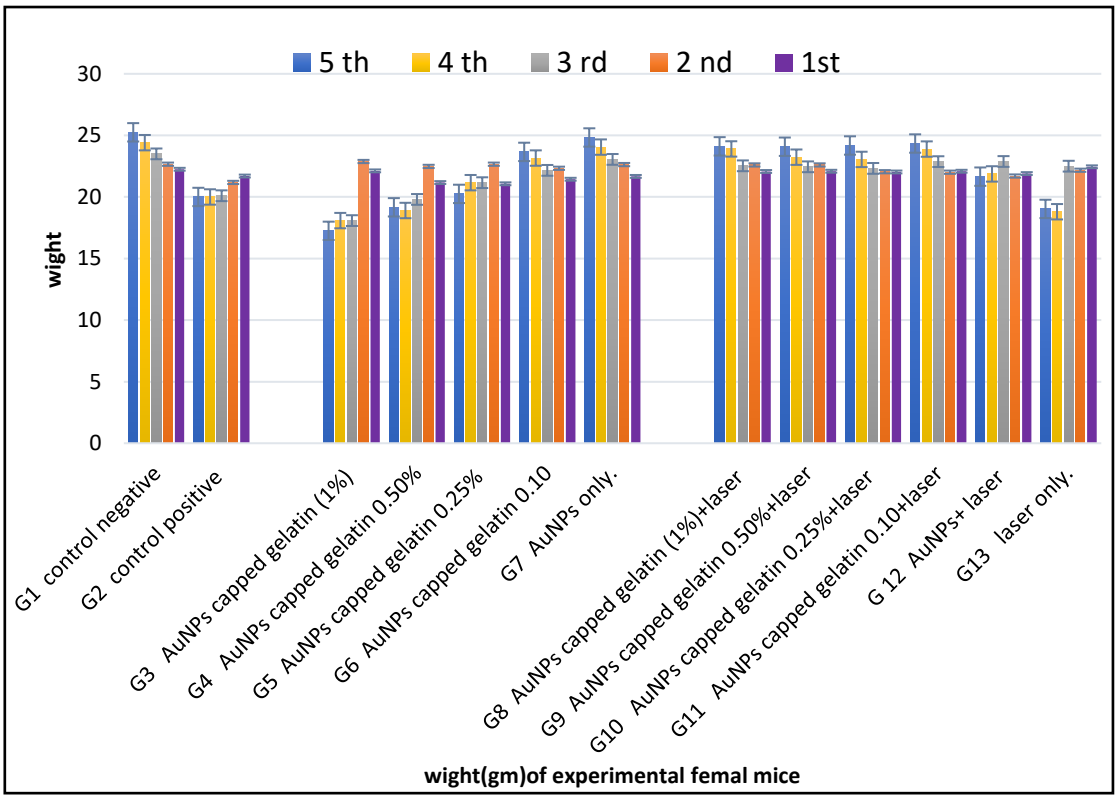

Figure 4 depicts the impact of PDT on the body weight (grams) of experimental female mice during the duration of the five-week study

Effect of PDT on tumor volume and growth inhibition rate(GIR)

Control +ve (G 2)= (Tumor-bearing female mice):

As shown in figure (5), the effects of PDT caused the tumor volume of the treatment groups to drop and the growth inhibition to rise, but the tumor volume of the control (+ve) group rose in a time-dependent manner, showing that the tumor was aggressive.

Groups treated with PDT

The phototoxic effect was diminished and GIR was reduced when the amount of AuNPs-capped gelatin injected into the tumor was reduced by diluting the solution to 0.50 percent and 0.25 percent figure (5), reaching 92.43 % and 75.80 % respectively. Complete tumor eradication occurred after the fifth week of the experiment, and the tumor is no longer visible macroscopically. Tumor growth was also significantly slowed, and the difference between the two groups was significant, with a significant difference between treated and untreated controls ($P<0.05$).

Groups treated with AuNPs capped gelatin

At the level of significance (($P<0.05$), the tumor volume exhibited a considerable decline.) for the groups (G3, G4,G5,and G6) only at the 3rd week group injected intratumorally (I/T)

AuNPs capped gelatin inhibition observed at the 5th week after **AuNPs capped gelatin** Application for the all concentrations (1%,0.50%,0.25%,0. 10%), as shown in figure (5).

GIR for groups treated with AuNPs capped gelatin increased only until the third week, then decreased to (23.6 %, 16.16 %, 12.09 %, and 7.56 %) for (G3, G4, G5, and G6) respectively, resulting in increased tumor volume (8.08, 8.87, 9.3 and 9.78 mm3) for groups T+ 1% AuNPs capped gelatin , T+0.0.50% AuNPs capped gelatin and T+ 0.25% AuNPs capped gelatin ,T+0.10% AuNPs capped gelatin respectively as shown in figure (5).

Group of tumor-bearing mice treated with laser

Irradiation of tumor mass without AuNPs capped gelatin application (G13) could not induce any macroscopic growth inhibition during the period of the experiment (5 weeks), no statistical significant difference was observed in tumor growth inhibition rate in comparison with control + ve (G2) figure (5). Diode laser (532 nm) irradiation at power density 0.542 Joule\cm² for 60 min of exposure time without AuNPs showed a significant difference ($P<0.05$) when compared with treated groups G3, G4, G5and G6, figure (6) showed a maximum decrease in growth inhibition rate (1.228 %) in the group (G13) tumor-bearing mice treated with laser alone (T+L). The tumor volume in G13 dramatically grew, reaching (10.45 mm3) at that point, compared to the control G2, which had reached (10.58 mm^3) by the fifth week of the study figure (6).

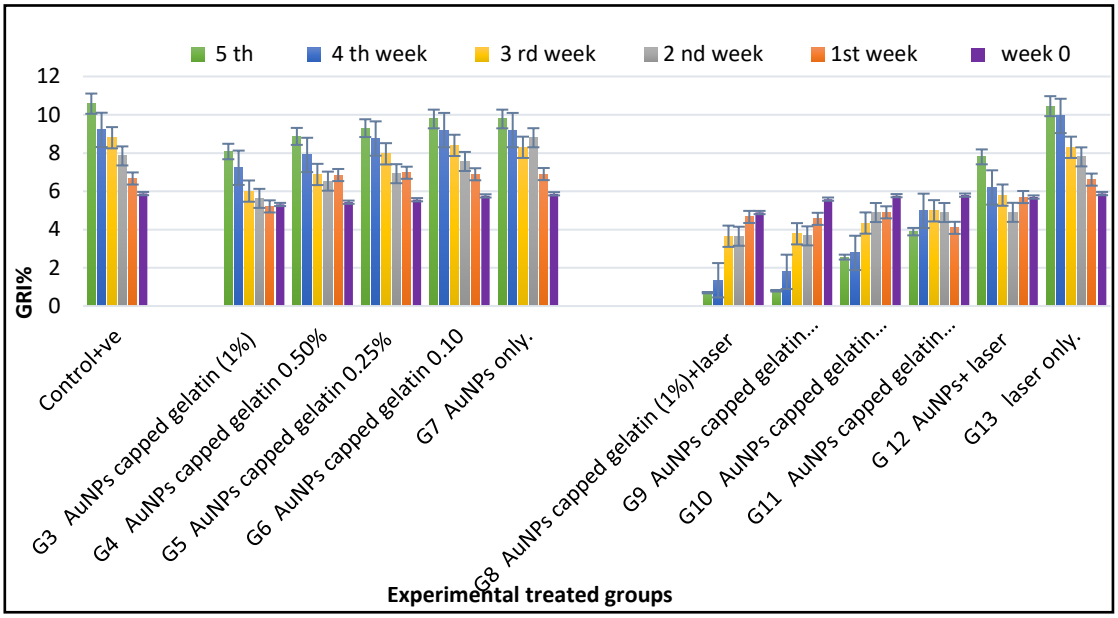

Figure.5 shows depicts, for each experimental group, the impact of PDT on tumor volume (mm3) during the course of the experiment's five weeks..

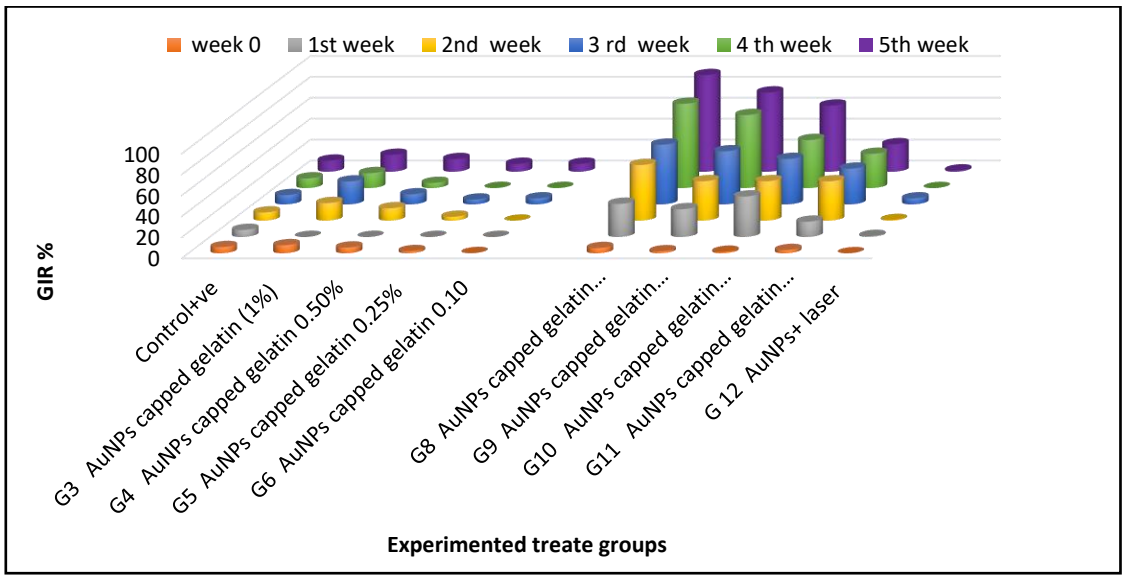

Figure .6 Effect of PDT on the growth inhibition rate of tumor volume during the five weeks of the experiment.

Statistical analysis

SPSS (version 24), a statistical package for social sciences, was used to perform the computations (for an examination of the specific significant differences

among groups). The data (proliferation or inhibition rates) were statistically analyzed using ANOVA and the post-hog Tukey test. P-values of 0.05 or less were deemed statistically significant.

Conclusion

In this paper, we presented a new method for preparing gold nanoparticles covered with gelatin, their sizes ranged between 10-20 nm. The optical properties depend on the concentration of gelatin. The highest concentration (1%) was found to have a small and more stable size.

It was found that the 532nm laser power using gelatin-coated gold nanoparticles as a photosensitizer to exert a phototoxic effect on cancer cells in vivo.

Increased the exposure period to 60 minutes using a diode laser at high power density after injecting 0.542 Joule/cm^2 ,1% AuNPs-capped gelatin intratumorally in mammary adenocarcinoma-bearing animals resulted in complete tumor elimination.

This is a fabricated procedure that involves coating AuNPs with gelatin. We believe that our research contributes to a useful way for determining the effect of AuNP size on concentration changes. Because of the difference in size of gold nanoparticles for the treatment of cancer tumors, this process can be adapted to create tiny size AuNPs or other noble metal nanoparticles.

References

S. Verma, P. Utreja, M. Rahman, and L. Kumar, "Gold Nanoparticles and their Applications in Cancer Treatment," Curr. Nanomedicine, vol. 8, no. 3, pp. 184–201, 2018, doi: 10.2174/2468187308666180312130055.

B. Khodashenas, M. Ardjmand, M. S. Baei, a. S. Rad, and a. a. Khiyavi, "Gelatin–Gold Nanoparticles as an Ideal Candidate for Curcumin Drug Delivery: Experimental and DFT Studies," in Journal of Inorganic and Organometallic Polymers and Materials, Vol. 29, No. 6, Springer US, 2019, Pp. 2186–2196. Accessed 8 Nov. 2022.

L. a. Dykman and N. G. Khlebtsov, "Gold Nanoparticles in Biology and Medicine: Recent Advances and Prospects," in Acta Naturae, Vol. 3, No. 2, 2011, Pp. 34–55. Accessed 8 Nov. 2022.

M. Sharon, A. Mewada, N. Swaminathan, and C. Sharon, "Synthesis of Biogenic Gold Nanoparticles and its Applications as Theranostic Agent: A Review," in Nanomedicine and Nanotechnology Journal, vol. 1, no. 1, 2017, p. 113.

M. P. Neupane et al., "Synthesis of gelatin-capped gold nanoparticles with variable gelatin concentration," in Journal of Nanoparticle Research, vol. 13, no. 2, 2011, pp. 491–498.

R. Yasmin, M. Shah, S. a. Khan, and R. Ali, "Gelatin Nanoparticles: A Potential Candidate for Medical Applications," in Nanotechnology Reviews, Vol. 6, No. 2, 2017, Pp. 191–207. Accessed 8 Nov. 2022.

K. Sztandera, M. Gorzkiewicz, and B. Klajnert-Maculewicz, "Nanocarriers in photodynamic therapy—in vitro and in vivo studies," in Wiley Interdisciplinary Reviews: Nanomedicine and Nanobiotechnology, vol. 12, no. 3, 2020, pp. 1–24.

K. Bromma and D. B. Chithrani, "Advances in Gold Nanoparticle-based Combined Cancer Therapy," Nanomaterials, Vol. 10, No. 9, Pp. 1–25, 2020, Doi: 10.3390/nano10091671. Accessed 8 Nov. 2022.

M. Q. Mesquita, C. J. Dias, S. Gamelas, M. Fardilha, M. G. P. M. S. Neves, and M. A. F. Faustino, "An insight on the role of photosensitizer nanocarriers for photodynamic therapy," in Anais da Academia Brasileira de Ciencias, vol. 90, no. 1, 2018, pp. 1101–1130.

A. Alhussan, E. P. D. Bozdoğan, and D. B. Chithrani, "Combining gold nanoparticles with other radiosensitizing agents for unlocking the full potential of cancer radiotherapy," Pharmaceutics, vol. 13, no. 4, 2021, doi: 10.3390/pharmaceutics13040442.

W. Yang, H. Liang, S. Ma, D. Wang, and J. Huang, "Gold nanoparticle based photothermal therapy: Development and application for effective cancer treatment," in Sustainable Materials and Technologies, vol. 22, 2019, pp. 1–29.

X. Huang, "Gold Nanoparticles Used in Cancer Cell Diagnostics, Selective Photothermal Therapy and Catalysis of NADH Oxidation Rezction," Technology, 2006.

M. S. Kang, S. Y. Lee, K. S. Kim, and D. W. Han, "State of the Art Biocompatible Gold Nanoparticles for Cancer Theragnosis," in Pharmaceutics, Vol. 12, No. 8, 2020, Pp. 1–22. Accessed 8 Nov. 2022.

X. Huang, P. K. Jain, I. H. El-Sayed, and M. A. El-Sayed, "Plasmonic photothermal therapy (PPTT) using gold nanoparticles," Lasers Med. Sci., vol. 23, no. 3, pp. 217–228, 2008, doi: 10.1007/s10103-007-0470-x.

D. Nath and P. Banerjee, "Green Nanotechnology - a New Hope for Medical Biology," in Environmental Toxicology and Pharmacology, Vol. 36, No. 3, Elsevier B.V., 2013, Pp. 997–1014. Accessed 8 Nov. 2022. [16] S. Nie, Y. Xing, G. J. Kim, and J. W. Simons, "Nanotechnology applications in cancer," Annu. Rev. Biomed. Eng., vol. 9, pp. 257–288, 2007, doi: 10.1146/annurev.bioeng.9.060906.152025.

F. Sanchez and K. Sobolev, "Nanotechnology in concrete - A review," in Construction and Building Materials, vol. 24, no. 11, 2010, pp. 2060–2071.

N. Y. Yaseen, "The Effect of Crude Extracts of Sonchus oleraceus on Cancer Cell Growth (In vitro) ايلاخلا ومن سمع ري رملا ريثأت تابنل ماخلا تاصمختسل ا جاجزلا (Sonchus oleraceus) يف قيناطرسلا," vol. 34, pp. 30–38, 2010.

F. M. Schabel, "p," no. February, 1984, pp. 717–726.